Hindawi
Advances in Materials Science and Engineering
Volume 2022, Article ID 6760385, 13 pages
https://doi.org/10.1155/2022/6760385

Research Article

Durability Performance of Concrete with Fly Ash as Fine Aggregate Eroded by Chloride Salt

Mingjie Mao,[1] **Qingyi Ai**,[1] **Dongsheng Zhang**,[2] **Sen Li**,[1] **and Jiabin Li**[2]

[1]*School of Civil and Hydraulic Engineering, Ningxia University, Yinchuan 750021, China*
[2]*Research Group RecyCon, Department of Civil Engineering, KU Leuven, Campus Bruges, 8200 Bruges, Belgium*

Correspondence should be addressed to Dongsheng Zhang; dongsheng.zhang@kuleuven.be

Received 14 November 2021; Revised 29 January 2022; Accepted 1 March 2022; Published 25 March 2022

Academic Editor: Robert Černý

The aim of this study is to investigate the durability of concrete with fly ash as a fine aggregate (CFA) in chloride salt environments. The natural diffusion method is used to analyze the concrete strength, chloride ion concentration, and diffusion coefficient after chloride salt erosion in a laboratory environment. In addition, scanning electron microscopy, X-ray diffraction, and Mercury intrusion porosimetry are performed to clarify the deterioration mechanism of concrete in chloride salt environments. The results indicate that owing to the chloride ion binding effect, the concrete porosity decreases and the concrete strength increases after chloride salt immersion. The decreased porosity caused by delayed hydration is primarily due to Friedel's salt and $CaCO_3$ produced during chloride ion erosion. CFA has a lower chloride diffusion coefficient and lower chloride concentration compared with ordinary concrete at all depths. In general, CFA exhibits excellent resistance to chloride salt erosion.

1. Introduction

The significant accumulation of fly ash not only causes environmental issues, but also poses a threat to human health [1]. China is the top producer of fly ash worldwide [2]. The low fly ash use efficiency and significant emissions by China have significantly deteriorated the surrounding water quality and atmosphere. Therefore, effective techniques should be developed to utilize fly ash in the construction field. In recent years, the research and application of fly ash in concrete technology have progressed considerably [3].

In chloride salt environments, steel corrosion is the primary factor that affects the durability of concrete structures. Chloride ions diffuse through concrete crack channels deep into the reinforcing steel surface, thereby damaging the passivation films on the surface [4–6]. When concrete structures are exposed to marine or deicing salt environments for long periods, chloride ions penetrate into the concrete, causing the reinforcement to corrode. This action decreases the effective bearing area of the reinforcing steel. Furthermore, the volume expansion caused by corrosion facilitates the cracking of the concrete protective layer, thereby ultimately reducing the bearing capacity and shortening the service life of the concrete structure [7].

Improving the pore structure and reducing the chloride penetration rate in concrete are effective measures to prolong the service life of reinforced concrete structures. Scholars have conducted extensive research regarding the application of fly ash concrete in chloride environments. It is concluded that fly ash can improve the internal porosity of concrete and increase its density. The partial replacement of cement with fly ash delays the depassivation of steel reinforcement, decelerates corrosion [8, 9], and improves the performance of concrete against chloride salt erosion.

Free chloride ions in the concrete pore solution, which destroy the passive film of the reinforcing steel and result in steel corrosion, are detrimental to concrete, not the total amount of chloride ions [10]. C_3A and C_4AF in cement can chemically react with chloride ions to produce Friedel salts and calcium chloride oxide ($Ca_3Cl_2O_2$) [11], and the hydration product, calcium silicate hydrate (C–S–H) gel, generates an adsorption effect on chloride ions. This can effectively reduce the harmful chloride ions in concrete via a reaction with Friedel salts and $Ca_3Cl_2O_2$ [10]. The service life of reinforced

concrete structures can be increased by 50%–200% owing to the chloride binding effect [12]. Glass et al. [13] discovered that the binding capacity of chloride ions increased with C_3A content, even when different cement types were used. When the C_3A content was increased from 2.43% to 14%, the chloride ion concentration threshold required for reinforcing steel corrosion increased by 2.85, which significantly delayed corrosion [14]. However, factors such as mineral admixtures, temperature, and chloride salt solution concentration can affect the chloride binding capacity of concrete [15]. Fly ash and other mineral admixtures are widely used in concrete applications. Studies [16–18] have shown that the partial replacement of cement with fly ash improves the chloride binding capacity. Cheewaket et al. [16] investigated the free and total chloride ion contents of concrete produced with fly ash at 0%–50% substitution rates using water- and acid-soluble methods; they discovered that by increasing the fly ash content, the chloride ion binding capacity increased, whereas the free chloride content decreased, thereby retarding the corrosion of reinforcing steel.

The concrete mix proportion, material type, and other factors affect the formation of the internal microstructure of concrete during hardening; consequently, resistance to the chloride penetration of concrete is affected [19]. The microstructure of concrete must be examined to reveal the material properties including the permeability [20]. The resistance of concrete to chloride ion attack provides a visual response to changes in its internal microstructure. Changes in the microstructure directly affect the macroscopic mechanical properties and durability of concrete [21]. Fly ash considerably affects the composition and microstructure of concrete hydration products [22]. The volcanic ash reaction densifies the concrete matrix, and the ash reacts with calcium hydroxide during cement hydration to produce additional C–S–H and calcium aluminate hydrate (C–A–H), thereby reducing the concrete porosity and optimizing the internal microinterface. Consequently, a dense matrix is generated, and a high-strength material that resists chloride ion diffusion into the concrete interior is formed [23, 24].

The time at which steel bar rusting is initiated and the rusting degree depend on the diffusion coefficient of chloride ions [25]. Researchers have applied Fick's second diffusion law to describe chloride ion diffusion in concrete [26]. The parameters of Fick's second diffusion law model provide a clear physical interpretation and can be used effectively to simulate existing test results [27]. Fly ash slightly affects the diffusion coefficient of chloride ions in early age concrete [28]. However, with extended exposure time, it significantly affects the diffusion coefficient of chloride ions. In later exposure stages, fly ash can significantly decrease the diffusion rate of chloride ions in concrete. Fly ash decreases the diffusion coefficient of chloride ions by 15%–50% [29, 30], thereby extending the expected service life of concrete structures. An optimal limit exists when using fly ash as a partial replacement for cement [31, 32]. When the replacement rate of fly ash exceeds the optimal value, the diffusion coefficient increases, which adversely affects the diffusion properties of anti-chlorine ions [33].

The relationship between the chloride diffusion coefficient and pore structure characteristics must be clarified to effectively reduce the chloride diffusion coefficient. Studies regarding the microstructure of fly ash concrete indicate that fly ash can refine the internal pore structure. When fly ash was used, the number of large pores decreased [21], the number of fine pores increased, and the total porosity and average pore size decreased significantly, thereby enhancing the resistance of concrete to chloride ion attack [22].

However, the positive effect of fly ash as a cement replacement material is limited. Seo et al. [34] recommend using fly ash as a partial replacement of fine aggregate (CFA), where some of the fly ash serves as a cementitious material with a volcanic ash effect, with the remainder having a microaggregate effect. CFA exhibits higher early age strength than fly ash concrete [35].

Most of the studies above pertain to the chloride ion binding and diffusion coefficients of fly ash concrete. Meanwhile, studies that investigate the performance of CFA in chloride salt environments are scarce. In this study, a laboratory natural diffusion method was adopted to investigate the durability of CFA in chloride salt environments. The chloride ion content at different depths was determined using chemical methods, and the chloride ion diffusion coefficient was determined based on Fick's second law of diffusion. The deterioration mechanism of concrete in chloride salt environments was determined using microstructural analysis techniques (SEM, MIP, and XRD). The technique of using CFA to prevent chloride salt erosion was investigated from macroscopic and microscopic perspectives, thereby promoting the development of concrete materials for environmental protection and high performance.

2. Materials and Methods

2.1. Materials. The binder was Grade P·O 42.5 ordinary Portland cement. The fine aggregate used for the tests was the middle sand of the second zone, which had a good assembly and distribution with an apparent density of 2600 kg/m^3 and a fineness modulus of 2.71. The coarse aggregate was a continuous collection of 5~20 mm natural crushed stone with an apparent density of 2700 kg/m^3, a crushing index of 10.2%, and a needle-like content of 9.7%. The fly ash was Grade III, and its chemical composition and physical properties are listed in Tables 1 and 2.

2.2. Experimental Design. The design standard value of concrete strength was C45, and the water–cement ratio was 0.42 (OPC). For the same water–cement ratio, the same fly ash volume was used to replace the fine aggregates to form CFA. The replacement percentages of fly ash were 10%, 20%, 30%, and 40%, and the corresponding serial numbers were denoted as CFA-10, CFA-20, CFA-30, and CFA-40, respectively, as shown in Table 3. Equation (1) was used to calculate the unit consumption of fly ash in concrete.

$$m_{\mathrm{FA}} = \frac{m_s \times w \times \rho_{\mathrm{FA}}}{\rho_S}, \tag{1}$$

Table 1: Chemical composition of fly ash.

Oxide	SiO_2	Al_2O_3	CaO	Fe_2O_3	MgO	SO_3	P_2O_5	Na_2O	K_2O
Content (%)	50.35	29.65	5.85	6.61	1.83	1.72	1.13	0.27	1.42

Table 2: Physical properties of fly ash.

Properties	Measured value
Fineness (% retained at 45 μm sieve)	34.3
Water demanded (%)	97
Loss on ignition (%)	5.7
Density (kg/m^3)	2130

Table 3: Concrete mix ratio at different replacement rates.

Sample	Water (kg/m^3)	Cement (kg/m^3)	Fly ash (kg/m^3)	Fine aggregate (kg/m^3)	Coarse aggregate (kg/m^3)
OPC	160	380	0	796	1100
CFA-10	160	380	64	716	1100
CFA-20	160	380	127	637	1100
CFA-30	160	380	192	557	1100
CFA-40	160	380	255	478	1045

where ρ_s and ρ_{FA} are the densities of the fine aggregate and fly ash (kg/m^3), respectively, and m_s and m_{FA} are the unit consumption of the fine aggregate and fly ash (kg), respectively.

2.3. Concrete Specimen Preparation and Casting. Based on the mix ratios, 100 mm × 100 mm × 100 mm cube specimens and 100 mm × 100 mm × 400 mm prismatic specimens were prepared. The cube specimens were used to determine the compressive strength of the CFA, whereas the prismatic specimens were used to determine the chloride ion content. After 24 h, the molds were removed and moved to a standard curing room for curing at 20 ± 2°C and relative humidity ≥95%. After curing for 28 days, the specimens were removed from the curing room. The top surface, bottom surface, and two small sides were sealed with epoxy resin to ensure one-dimensional diffusion of chloride ions into the concrete. The specimens were immersed in NaCl solutions with mass concentrations of 0%, 1.5%, 3.5%, and 5% and subjected to compressive strength and chloride ion content tests after chloride salt immersion for 90 d.

2.4. Test Method. After the concrete specimens were immersed in the corrosive solution and corroded for 90 days, they were removed from the solution. The compressive strengths of the cube specimens were then determined [36] (Figure 1).

Samples were obtained from the two sides of the prismatic specimen using the drilling method (Figure 2(a)). A small drilling machine with a drill bit diameter of 8 mm was used for drilling. Powder samples were obtained layer by layer along the erosion surface every 1, 2, and 5 mm within depths of 10, 10–20, and 20–30 mm, respectively. The free chloride ion content (C_f) and total chloride ion content (C_t) in each sample were determined via chemical titration (Figure 2(b) and 2(c)) based on JTJ 270–98 [37].

3. Results and Discussion

3.1. Compressive Strength. The compressive strength results of CFA after soaking in different salt solutions are presented in Figure 3(a). The growth rate of strength relative to immersion in water is shown in Figure 3(b).

As the replacement rate of fly ash increased, the CFA strength increased gradually. Under 1.5% and 3.5% NaCl solution concentrations, the CFA-40 group exhibited the highest strength, i.e., 75.8 and 77.8 MPa, respectively. When immersed in the 5% NaCl solution concentration, the compressive strength of the CFA-30 group increased only slightly, i.e., reaching 80.9 MPa, compared with that of the CFA-40 group. In the typical fly ash concrete, the $Ca(OH)_2$ content in the hydration products decreases as the fly ash content increases and does not fully participate in the volcanic ash reaction. Moreover, a significant amount of unhydrated fly ash glass in the concrete is expelled during the convection of the internal and external media, thereby increasing the concrete porosity. For CFA, fly ash replaces the fine aggregates in OPC, and the cement quantity remains the same. Hence, the active ingredients in fly ash can fully react with the $Ca(OH)_2$ of cement hydration products, thereby inducing a zeolite reaction and generating a C–S–H gel that can fill the internal pores of the concrete. Furthermore, fly ash exhibits the characteristics of small particles and has a large specific surface area. Hence, it can fill the large pores between the cement and aggregate particles and exhibit an excellent microaggregate filling effect, thereby densifying the concrete.

Figure 3(b) shows the growth rate of compressive strength. Longitudinally, as the salt concentration increased, the concrete strength increased to some extent. The growth rates of compressive strength in the 1.5%, 3.5%, and 5% salt solutions were approximately 5.5%, 8.8%, and 11.4%, respectively, which were within the 15% error range. The concrete in the chloride salt environment due to the chloride ion binding effect increased the concrete strength, although the increase was insignificant. In the short term, chloride salts can promote the development of concrete strength. The intrusion of chloride ions, which results in the corrosion of the reinforcement, is a more important subject.

3.2. Chloride Ion Concentration. The chloride ions are divided into bound and free chloride ions. The latter play a decisive role in the corrosion process of steel reinforcement and are widely recognized as such.

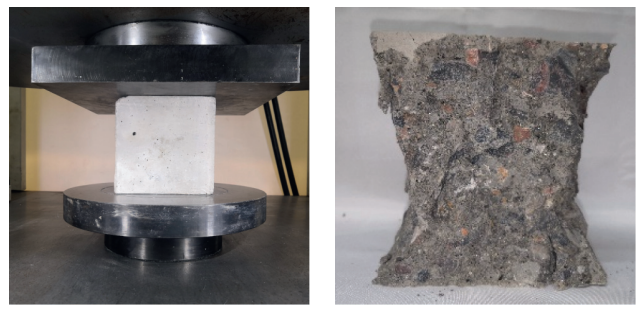

(a) (b)

Figure 1: Loading method and breaking patterns. (a) Schematic diagram of compressive loading. (b) Compression damage pattern.

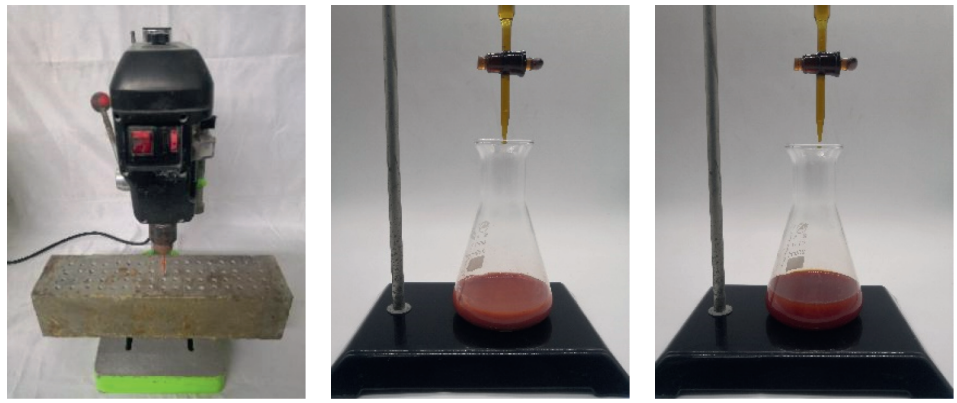

(a) (b) (c)

Figure 2: Diamond powder sampling and titration. (a) Sampling. (b) Total chloride ion titrated to red. (c) Free chloride ion titrated to brick red.

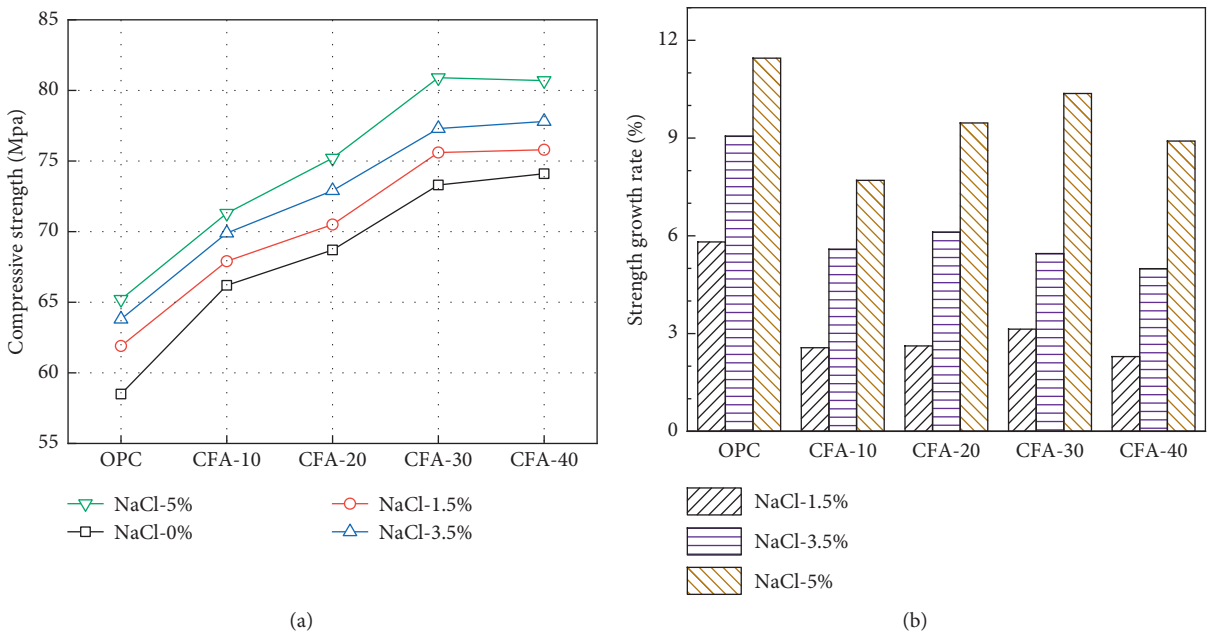

(a) (b)

Figure 3: Compressive strength and growth rate of CFA. (a) Compressive strength. (b) Strength growth rate.

In a laboratory environment, the natural diffusion method can be applied to investigate the diffusion behavior of chloride ions in concrete, and precisely reflect the combination and diffusion characteristics of concrete and chloride ions [38].

The distributions of the free chloride ion concentration of CFA containing different fly ash contents are shown in Figure 4. The concentration of free chloride ions at each depth in each concrete group increased gradually with the salt solution concentration. The chloride ion concentrations at different depths of the CFA with varying fly ash contents were lower than those of the control concrete. The penetration depth of the chloride ions increased gradually with the salt solution concentration, and a free chloride ion concentration of up to 0.02% (mass fraction) was adopted as an index to evaluate the penetration depth of CFA. The penetration depths of the OPC and CFA-40 concrete specimens in the 1.5% NaCl solution were 16 and 11 mm, respectively. When the salt solution concentration was increased to 5%, the corresponding penetration depths increased to 20 and 18 mm, respectively. This difference was caused by the increased salt solution concentration and increased gradient difference between the internal and external chloride ion concentrations, which induced the chloride ion diffusion effect. The distance at which chloride ions underwent directional migration increased at high chemical potential gradients.

Figure 5 shows the trend of the total chloride ions at different salt solution concentrations. In the 5%, 3.5%, and 1.5% NaCl solution immersion environments, the free chloride ion concentrations at a 1 mm depth from the surface were 0.85%, 0.75%, and 0.55%, respectively, whereas the total chloride ion concentrations were 0.87%, 0.80%, and 0.61%, respectively. This behavior is attributed to the chloride ion binding properties. The trends for the total and free chloride ion contents in the three different salt solution concentrations were similar, and the variations in the free and total chloride ion concentrations with depth were exponential.

The free and total chloride ion contents at different depths decreased gradually as the replacement rate of fly ash increased. The resistance of CFA to chloride ion penetration peaked at a fly ash content of 40%. First, the small size of the fly ash particles enhanced the compactness of the cementing materials, thereby improving the filling and impermeability of the concrete. Second, the volcanic ash effect of the fly ash reduced the less stable $Ca(OH)_2$ content, optimized the slurry structure, and improved the resistance of concrete to chloride ion attack [39]. The high Al_2O_3 content of fly ash accelerated the generation of chloride ion-binding Friedel salts and increased the bound chloride ion content. Therefore, it significantly improved the resistance of concrete to chloride salt attack.

3.3. Chloride Ion Binding Capacity. The measured free and total chloride ion contents were used to calculate the binding capacity, R, of chloride ions to concrete. Nilsson et al. [40] defined the chloride binding capacity, R, as follows:

$$R = \frac{\partial C_b}{\partial C_f} = \frac{\partial \left(C_t - C_f\right)}{\partial C_f}, \tag{2}$$

where R is the chloride ion binding capacity, C_b is the bound chloride ion content (%), and C_f is the free chloride ion content (%).

The R values of the chloride binding capacity for different fly ash replacement rates are shown in Figure 6. A weak correlation between chloride salt concentration and binding capacity was observed. The binding capacity values for OPC immersed in the 5%, 3.5%, and 1.5% salt solution concentrations were 0.101, 0.105, and 0.109, respectively; i.e., the values increased slightly as the salt solution concentration increased.

The chloride ion binding capacity of CFA increased gradually with the fly ash content, and that of the CFA with 40% fly ash reached approximately 0.42. Studies [15, 16] show that the chloride ion binding capacity of fly ash concrete ranges from 0.15 to 0.25, whereas that of CFA ranges from 0.15 to 0.42, which is significantly higher than that of fly ash concrete in the current study.

The chloride binding capacity of concrete depends on physical adsorption and chemical bonding, in which chloride ions react with C_3A to yield calcium chloroaluminate hydrate ($C_3A{\cdot}CaCl_2{\cdot}10H_2O$), known as Friedel's salt [41], which retards the rate of chloride ion penetration. The aluminium phase content of the raw material is vital to the binding of chloride ions; among the contents, C_3A is positively correlated with the chloride ion binding ability. Moreover, C–S–H gels can absorb some chloride ions [42], and the secondary hydration reaction of fly ash produces additional C–S–H gels, which reduces the alkalinity of the internal pore solution of concrete, thereby increasing the physical adsorption capacity. Consequently, the binding property of CFA is more significant than that of fly ash concrete.

3.4. Chloride Ion Diffusion Coefficient. The erosion patterns of CFA produced with different fly ash contents immersed in different salt solution concentrations were examined. The obtained results were as expected, and for the specimens soaked in the NaCl salt solutions, the variation in the chloride ions with depth obeyed Fick's second law of diffusion. Fick's second law of diffusion [43] can be expressed as follows:

$$\frac{\partial C}{\partial t} = \frac{\partial}{\partial x}\left(D \cdot \frac{\partial C}{\partial x}\right). \tag{3}$$

The boundary conditions for the chloride ion diffusion in concrete can be expressed as follows:

$$C(x > 0, t = 0) = C_0, \quad C(x = 0, t \geq 0) = C_s. \tag{4}$$

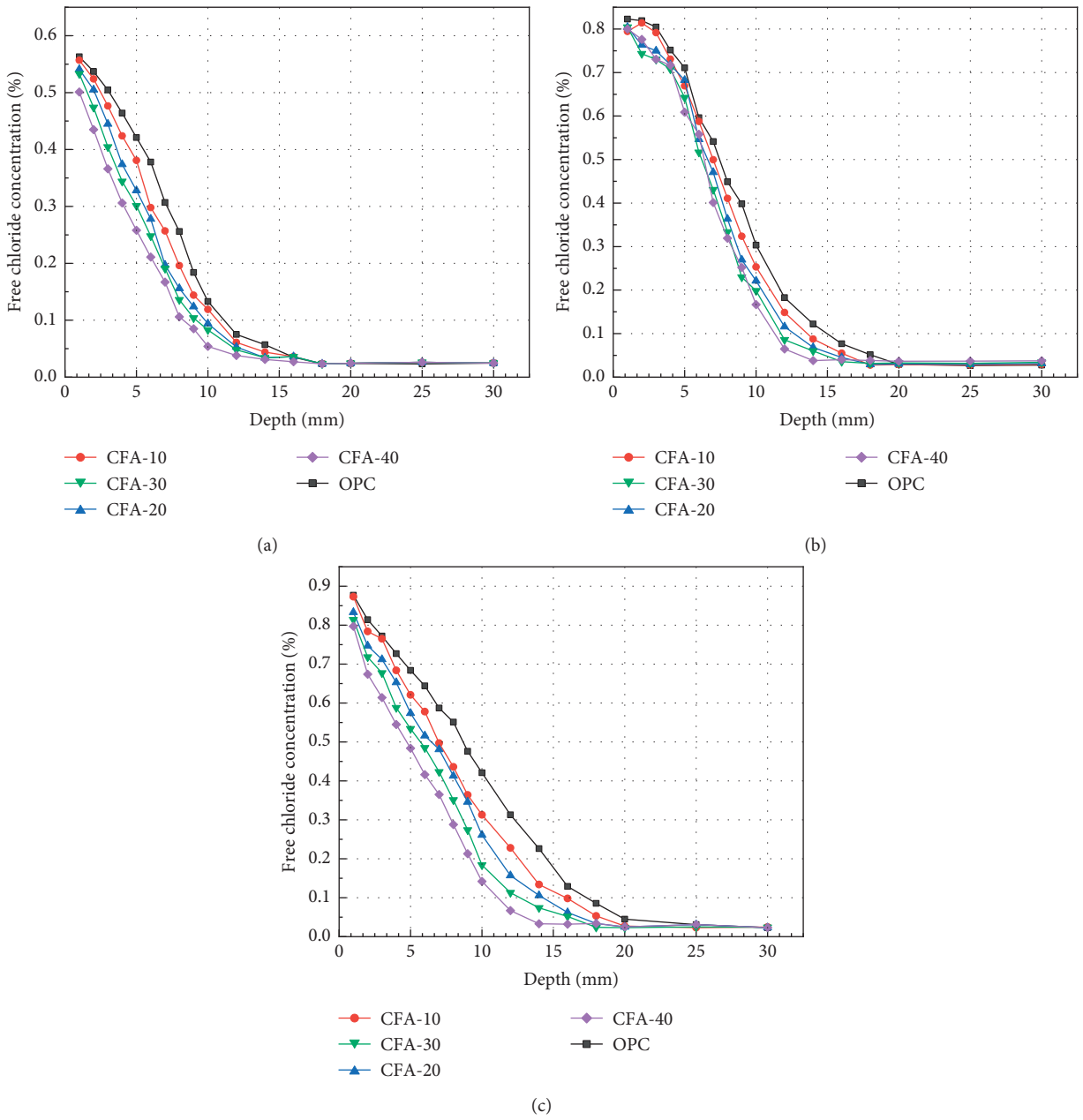

Figure 4: Variations in free chloride ion concentration with the depth of CFA. (a) NaCl-1.5%. (b) NaCl-3.5%. (c) NaCl-5%.

Bringing the boundary conditions into (3), we can find the following:

$$C(x,t) = C_0 + (C_s - C_0)\left[1 - erf\left(\frac{x}{2\sqrt{Dt}}\right)\right]. \quad (5)$$

The inverse solution of the diffusion coefficient leads to the derivation of the formula for the chloride ion diffusion coefficient as follows:

$$D = \frac{1}{t}\left(\frac{x}{2erf^{-}\left(1 - C(x,t) - C_0/C_s - C_0\right)}\right)^2, \quad (6)$$

where C_0 is the initial chloride ion concentration in concrete (an initial concentration of 0.0001% was assumed), C_s is the chloride ion concentration at the concrete surface (%), D is the chloride ion diffusion coefficient ($m^2 \cdot s^{-1}$), x is the distance between the erosion interface and the concrete surface (mm), t is the duration of the chloride ion diffusion (s), and *erf* is the Gaussian error function.

Figure 7 shows the fitted chloride ion diffusion coefficients. Highly concentrated salt solutions increase the possibility of chloride ion attack, and chloride ion diffusion increases accordingly as the salt solution concentration increases. The diffusion coefficients of chloride ions immersed in the 5% NaCl solution were generally higher than those in the 1.5% and 3.5% NaCl solutions. The diffusion coefficient of the OPC group in the 1.5% NaCl solution was $5 \times 10^{-12}\ m^2 \cdot s^{-1}$, and that of the CFA-40 group was

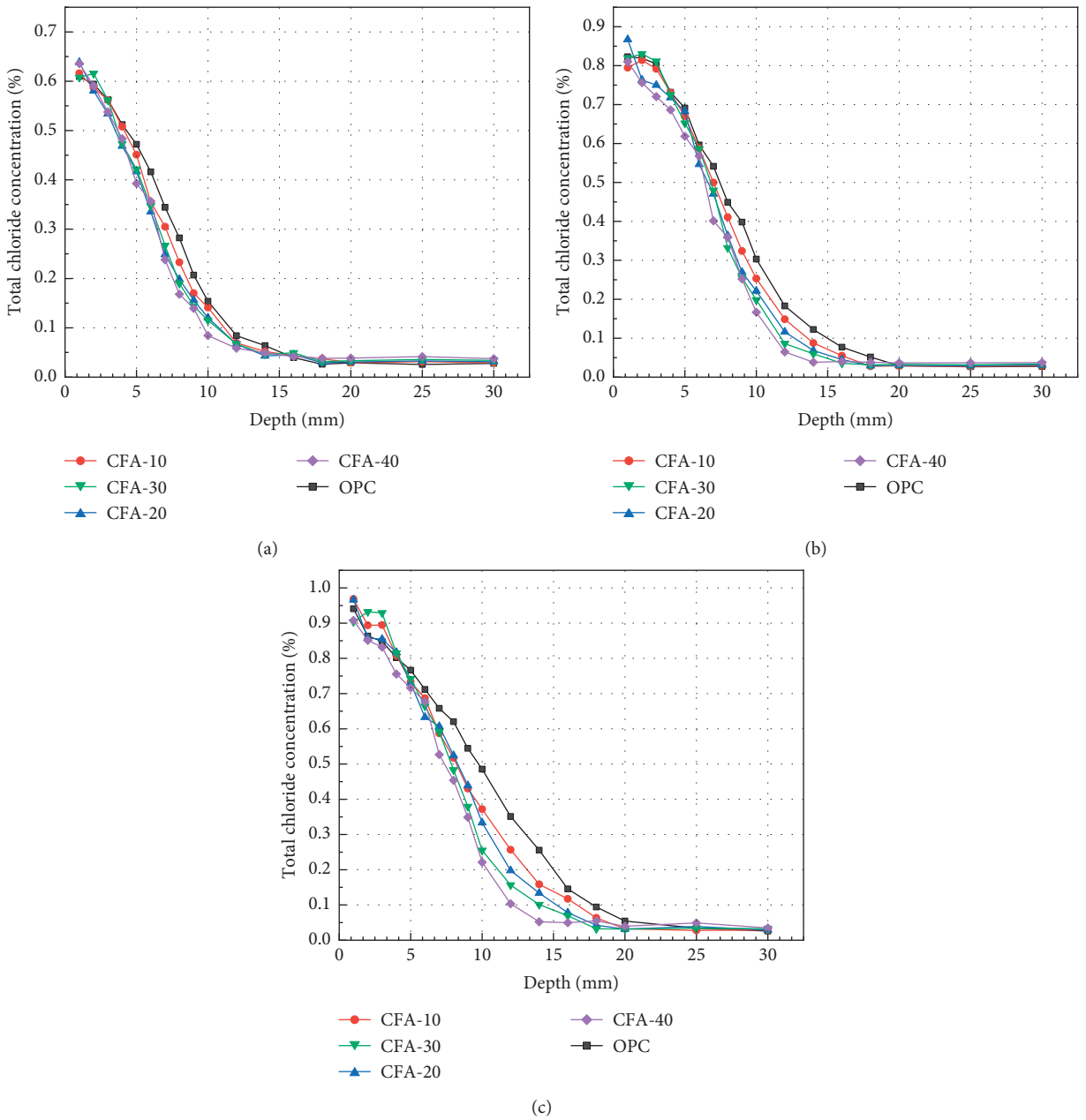

Figure 5: Variations in total chloride ion concentration with the depth of CFA. (a) NaCl-1.5%. (b) NaCl-3.5%. (c) NaCl-5%.

2.7×10^{-12} $m^2 \cdot s^{-1}$, which is a reduction by 46% compared with the OPC group. When the salt solution concentration was 5%, the OPC group specimens indicated a diffusion coefficient of 9.4×10^{-12} $m^2 \cdot s^{-1}$, whereas the CFA-40 group specimens indicated a diffusion coefficient of 3.9×10^{-12} $m^2 \cdot s^{-1}$. Although all the diffusion coefficient values increased in the highly concentrated salt solutions, the increasing degree was different. Specifically, the diffusion coefficients for the OPC and CFA-40 groups increased by 88% and 43%, respectively.

The CFA diffusion coefficient decreased gradually as the amount of blended fly ash increased. Compared with ordinary concrete, the chloride diffusion coefficients of the CFA-40 group specimens in the 1.5%, 3.5%, and 5% NaCl environments decreased by 58%, 46.1%, and 46%, respectively. This indicates that CFA with a 10%–40% replacement rate of fly ash is better than ordinary concrete in terms of resistance to chloride ion attack.

4. Microstructural Analysis

4.1. MIP. Concrete is a nonhomogeneous material whose pore characteristics influence its permeability. The classical seepage theory suggests that the pore structure of a material determines its permeability properties. MIP is generally used for determining pore size distribution. This method is widely used to characterize the total porosity and pore size distribution of concrete. The influence of the pore size

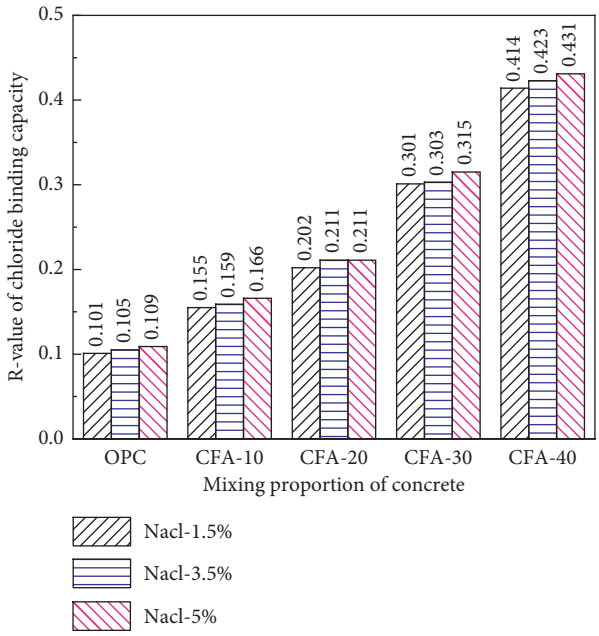

Figure 6: R values of chloride ion binding capacity.

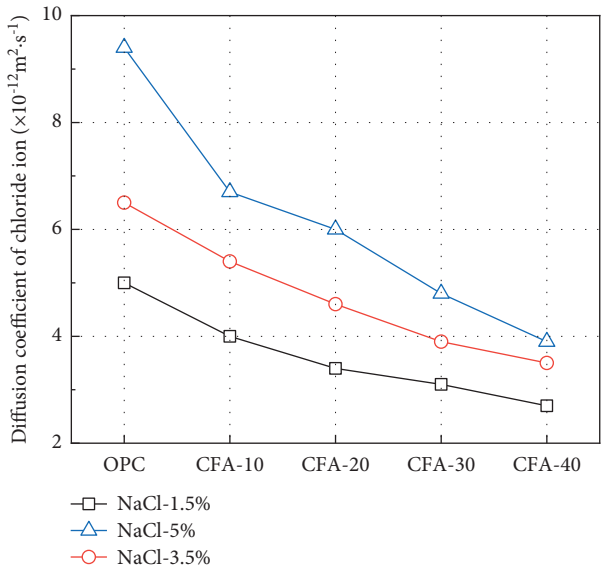

Figure 7: Diffusion coefficients of chloride ions.

distribution of CFA on the corrosion resistance to chloride ions was analyzed. In this study, the pore size of concrete is divided into four levels: < 20 nm (harmless pores), 20–50 nm (less harmful pores), 50–200 nm (harmful pores), and >200 nm (multi-harmful pores).

Figure 8 shows the differential log-aperture relationship curve. Compared with the OPC group concrete, the pores of the CFA-40 group concrete were smaller, and the proportion of small pores was higher. The most probable pore size for the OPC group decreased from 35.423 to 32.414 nm, and that of the CFA-40 group decreased from 34.876 to 32.141 nm. After soaking in the 3.5% NaCl salt solution, the pore sizes were redistributed, and the pore structure was optimized.

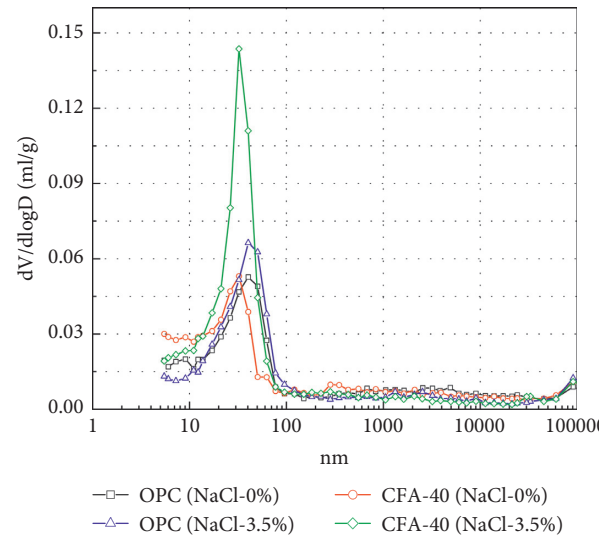

Figure 8: Differential logarithmic curves of Mercury intake.

The proportions of different pore sizes were calculated based on the MIP data (Figure 9). The percentages of <20 nm pores in the OPC and CFA-40 group specimens were 37.3% and 63.7% in clear water, respectively. The CFA specimens had lower porosity, more refined pore sizes, and higher density than the OPC concrete specimens; additionally, they exhibited a good pore structure.

After soaking in the 3.5% NaCl solution, the percentage of <20 nm pores in the OPC group specimens increased from 37.3% to 55.5%, and the percentage of 20–50 nm pores decreased from 43.9% to 34.9%. Correspondingly, the percentage of <20 nm pores in the CFA-40 group specimens decreased from 63.7% to 58.6%, but the percentage of 20–50 nm pores increased from 27.4% to 38.1% due to chloride binding properties. The <20 nm pores were filled gradually with more salt as the generated chemical products continued to increase and filled the pores; when the chemical binding products increased to a certain degree, the small pores ruptured. Consequently, the proportion of <20 nm pore size decreased after the immersion of CFA-40 in the 3.5% salt solution.

Figure 10 shows the pore characterization parameters obtained during the MIP analysis. In clear water, the average pore diameter of the CFA-40 group specimens was 33.7% lower than that of the OPC group specimens, and the total pore area increased. This increase indicates that the volume of large pores in CFA decreased, whereas the number of small pores increased; additionally, the pore system compactness improved, and the pore structure was refined and optimized. The optimized pore structure strengthened the concrete and rendered the concrete structure more resistant to chloride ion penetration.

After soaking in clean water, the porosity of the CFA-40 group specimens decreased by 2.68% compared with that of the OPC group specimens. The reduced porosity of CFA was caused by the fly ash microaggregate filling effect as well as the volcanic ash effect, although the former was dominant. In contrast to water immersion [44], the decrease in porosity after immersion in a salt solution is primarily attributed to

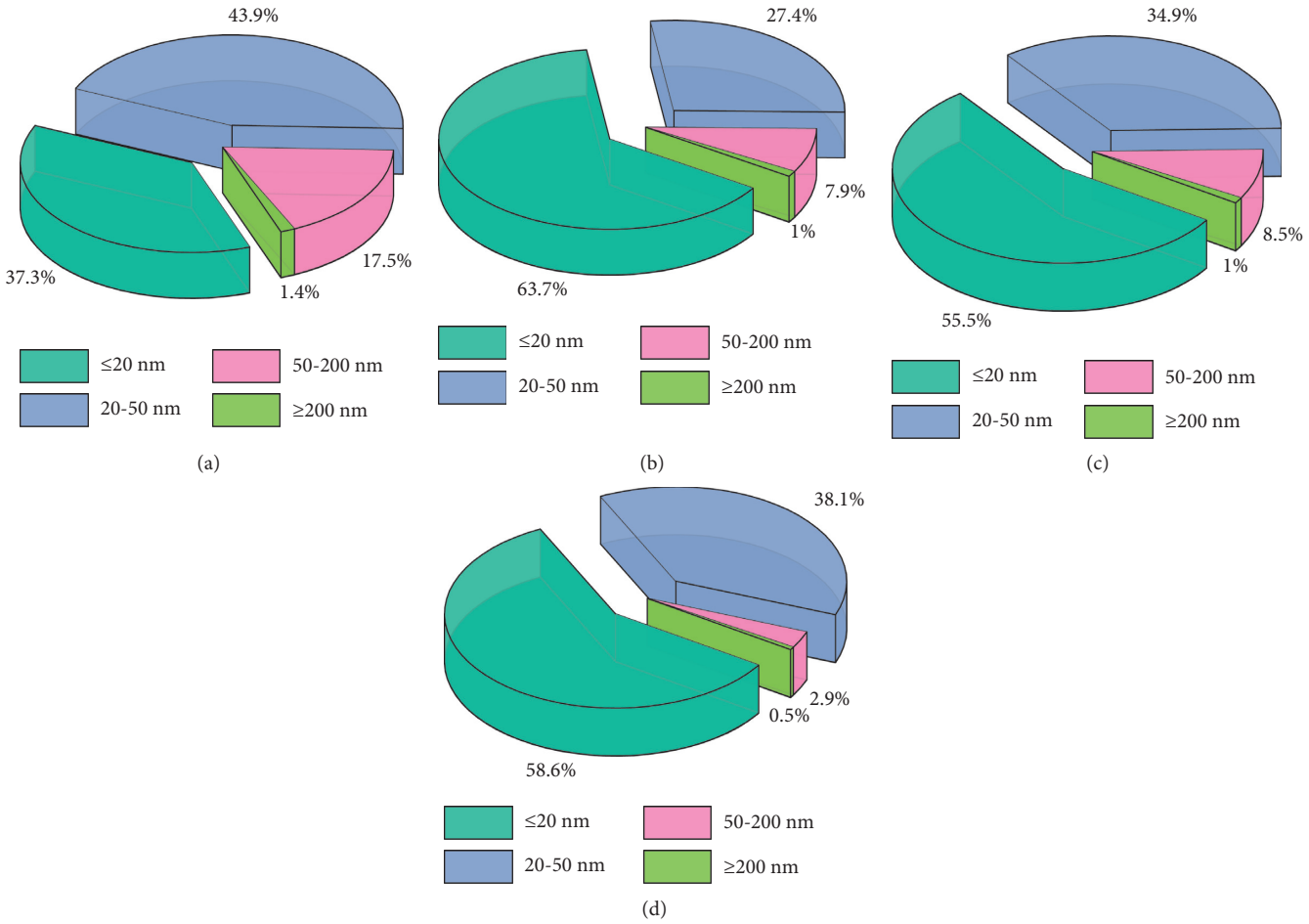

Figure 9: Proportion of pore sizes for each concrete group. (a) OPC (NaCl-0%). (b) CFA-40 (NaCl-0%). (c) OPC (NaCl-3.5%). (d) CFA-40 (NaCl-3.5%).

Friedel's salts, CaCO3, and other substances produced during chloride ion erosion.

4.2. XRD. Figure 11 shows the XRD patterns of the concrete specimens. The characteristic peaks of SiO_2 appeared in the diffraction spectra of each specimen, and the SiO_2 came from raw materials, such as the fly ash and coarse aggregate. Friedel's salt diffraction peak appeared near 11.2° in the concrete specimens after erosion by the NaCl salt solution; that is, Friedel's salt formed during the chemical reaction between the chloride ions and raw materials. The Friedel salt diffraction peak of the CFA containing 40% fly ash was more significant than that of the OPC group specimens.

The AFt diffraction peak appeared near 9°, and the AFt peak of the concrete specimen in the clear water was more significant than that in the 3.5% NaCl salt solution. There are different explanations for the weakening of the AFt peak. Zibara [45] suggested that in chloride salt solutions with high concentrations, AFt may be transformed to Friedel's salts, thus acting as a binding agent for chloride ions. Ekolu et al. [46] opine that AFt and AFm are destroyed to form Friedel's salts when the chloride ion concentration exceeds 0.5 mol/L (approximately 0.6 mol/L for a 3.5% NaCl solution by a mass fraction).

Compared to the concrete specimens immersed in clear water, the $Ca(OH)_2$ diffraction peak significantly decreased and the $CaCO_3$ diffraction peak increased after 90 days of immersion in the NaCl solution. The appearance of the Friedel salt diffraction peak was inevitably related to the strengths of the $Ca(OH)_2$ and $CaCO_3$ diffraction peaks. When the chloride ions penetrated the concrete, the following reaction occurred:

$$C_3A + Ca(OH)_2 + 2\mathrm{NaCl} + 10H_2O \longrightarrow 2Na + 2(OH)^- + \mathrm{Friedel} + SO_4^{2-} + 2H_2O. \quad (7)$$

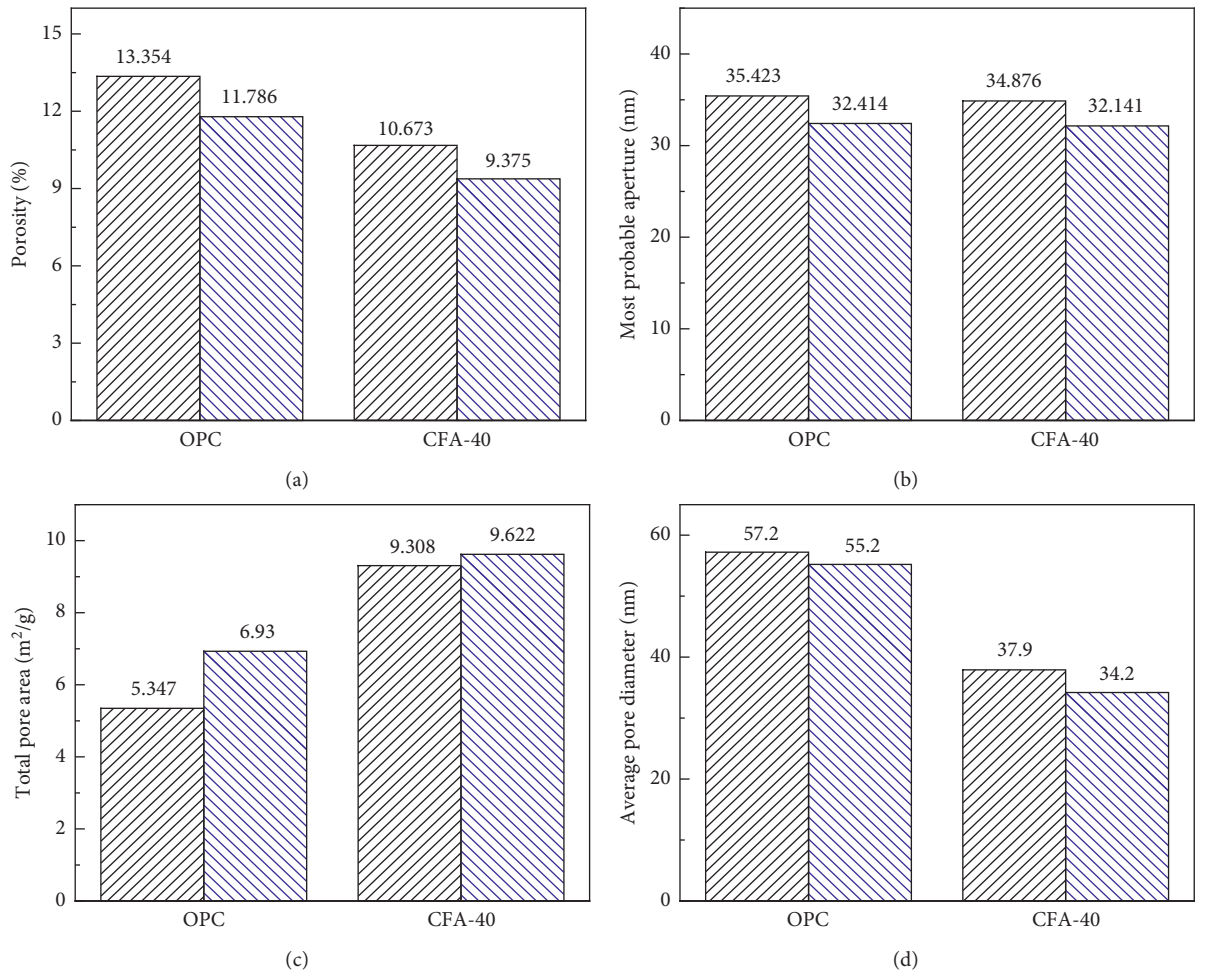

Figure 10: Pore characterization parameters (a) Porosity. (b) Most probable aperture. (c) Total pore area. (d) Average pore diameter.

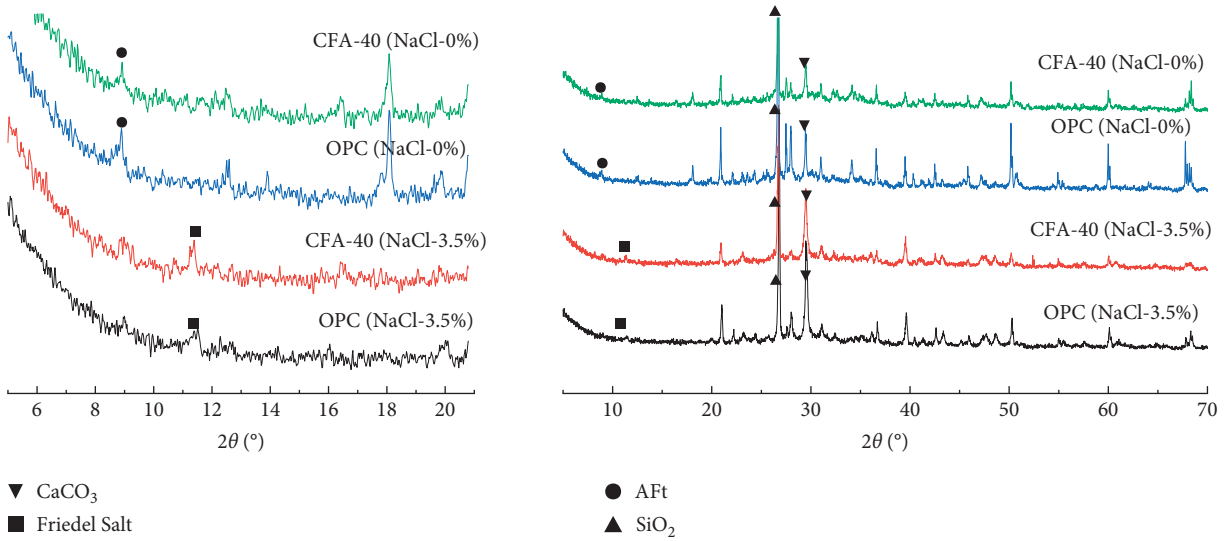

Figure 11: XRD patterns of concrete group specimens.

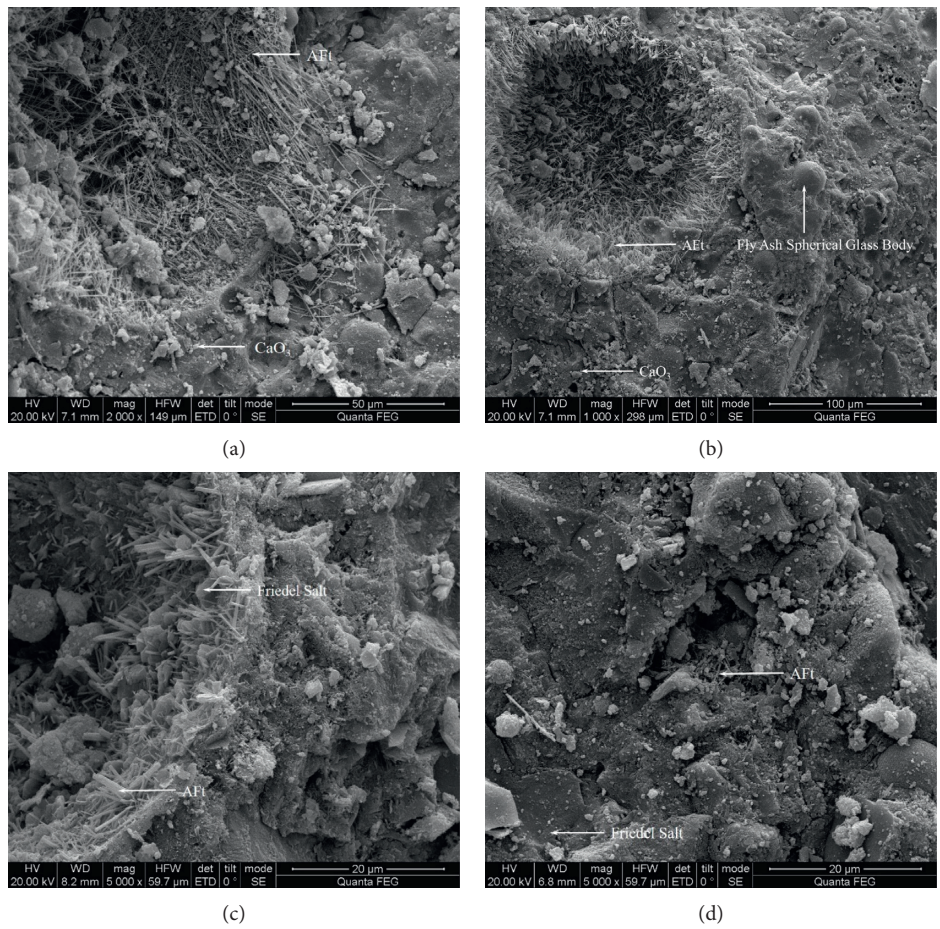

Figure 12: SEM images of concrete specimens. (a) OPC (NaCl-0%). (b) CFA-40 (NaCl-0%). (c) OPC (NaCl-3.5%). (d) CFA-40 (NaCl-3.5%).

CO_3^{2-}-AFm, CO_3^{2-}AFm, and HO^--AFm are all members of the AFm family, and all of them can be chemically bound to chloride ions. The chloride ion displaces CO_3^{2-}, CO_3^{2-}, and HO^- in the AFm phase, thus generating Friedel's salts. When CO_3^{2-} is replaced, it reacts to form $CaCO_3$, which is insoluble in water. Thus, the $CaCO_3$ diffraction peaks in the XRD patterns were significantly enhanced.

4.3. SEM. Figure 12 shows SEM images of the microscopic morphology of the concrete specimens. The hydration reaction of C_3A with gypsum produced the AFt phase because the raw materials contained gypsum. The OPC and CFA-40 group specimens produced many needle-like prismatic AFt phase crystals after soaking in water (Figure 12(a) and 12(b)). The high-concentration salt solution disrupted the AFt phase and combined with Cl^- to produce Friedel's salt hexagonal plates. Figures 12(c) and 12(d) show the microscopic morphology after immersion in the 3.5% NaCl salt solution. The AFt phase distribution of needle-like prismatic crystals was sparse, and the content was relatively small. Moreover, the formation of Friedel's salt was observed. CFA-40 group specimens had a spherical glass body of the unreacted fly ash with a layer of hydration products on the surface. Furthermore, the fly ash reduced the orientation of the concrete interface. Hence, the aggregate and paste formed a matrix, improving concrete impermeability.

5. Conclusions

In this study, the durability performance of CFA in a chloride salt environment was investigated. The following conclusions were obtained:

(1) The strength of the concrete specimens increased after they were immersed in chloride salt, where a higher chloride salt concentration resulted in higher concrete strength. With the use of microscopic analysis, it was evident that in the clear water group, the CFA strength increase was primarily dominated by the fly ash microaggregate filling effect. After salt solution erosion, the CFA strength increase was primarily due to the chloride ion binding effect, which generated salts (primarily F salt), $CaCO_3$, and other products inside the concrete. These materials filled the internal pores of the concrete and decreased the porosity of the concrete specimens.

(2) The chloride ion binding capacity correlated weakly with the chloride salt concentration but correlated strongly with the fly ash content. The chloride ion

aggregation capacity improved gradually as the fly ash content increased. The binding capacity of CFA containing 40% fly ash was 0.42. This value is significantly higher than that of fly ash cement concrete owing to the higher aluminium phase in CFA, which provided the components required to bind the chloride ions.

(3) The salt solution concentration affected the chloride ion concentration and diffusion coefficient at different depths of the concrete specimens. The higher the salt solution concentration, the greater the diffusion coefficient. The chloride ion diffusion coefficient and chloride ion concentration at different CFA depths were lower than those of the control concrete, and the resistance of CFA to chloride salt attack was significantly higher than that of the control concrete.

(4) After CFA was immersed in the chloride salt solution, Friedel's salt was generated because of the binding effect of chloride ions. The distribution of needle-like prismatic AFt phase crystals inside the concrete was sparse, and the content was relatively low. This might be because the high-concentration salt solution dissolved the AFt phase to generate AFm, and the chloride ions replaced CO_3^{2-} in the AFm phase. Hence, Friedel's salt was generated, which subsequently reacted with Ca+ to yield $CaCO_3$ (which is insoluble in water), thereby increasing the $CaCO_3$ content.

(5) Concrete produced with fly ash fine aggregates exhibited low porosity and a good pore structure. Based on the test results, CFA exhibited high resistance to chloride ion attack.

Data Availability

The data used to support the findings of this study are available from the corresponding author upon request.

Conflicts of Interest

The authors declare that there are no conflicts of interest regarding the publication of this article.

Authors' Contributions

Dongsheng Zhang participated in conceptualization, methodology, formal analysis, data analysis, and resources; prepared the original draft; and revised and edited the paper. Qingyi Ai contributed to methodology, formal analysis, data analysis, and resources and prepared the original draft. Sen Li worked on investigation and visualization. Mingjie Mao helped with investigation, supervision, and project administration; prepared the original draft; and revised and edited the paper. Jiabin Li revised and edited the paper. All authors approved the final version of the paper.

Acknowledgments

This study was supported by the Graduate Innovation Project of Ningxia University (GIP2021-25); National Natural Science Foundation of China (Project No. 51768058); key R&D projects of Ningxia Province of China (Project Nos. 2021BEE03004 and 2021BEG02014); and construction project of joint training demonstration base for research, production, and teaching integration of Ningxia University. Their results were fundamental to this study.

References

[1] H. Ş. Arel and F. U. A. Shaikh, "Effects of fly ash fineness, nano silica, and curing types on mechanical and durability properties of fly ash mortars," *Structural Concrete*, vol. 19, no. 2, pp. 597–607, 2018.

[2] X. Gong, H. Yao, and D. Zhang, "Leaching characteristics of heavy metals in fly ash from a Chinese coal-fired power plant," *Asia-Pacific Journal of Chemical Engineering*, vol. 5, no. 2, pp. 330–336, 2010.

[3] A. M. Rashad, "An exploratory study on high-volume fly ash concrete incorporating silica fume subjected to thermal loads," *Journal of Cleaner Production*, vol. 87, pp. 735–744, 2015.

[4] T. Cheewaket, C. Jaturapitakkul, and W. Chalee, "Initial corrosion presented by chloride threshold penetration of concrete up to 10 year-results under marine site," *Construction and Building Materials*, vol. 37, pp. 693–698, 2012.

[5] Z. Jin, X. Zhao, T. Zhao, and Y. Liu, "Corrosion behavior of steel bar and corrosive cracking of concrete induced by magnesium-sulfate-chloride ions," *Journal of Advanced concrete Technology*, vol. 14, no. 2, pp. 172–182, 2016.

[6] J. Liu, F. Xing, B. Dong, H. Ma, and D. Pan, "Study on water sorptivity of the surface layer of concrete," *Materials and Structures*, vol. 47, no. 11, pp. 1941–1951, 2014.

[7] J. Bilcik and I. Holly, "Effect of reinforcement corrosion on bond behaviour," *Procedia Engineering*, vol. 65, pp. 248–253, 2013.

[8] C. Zou, G. Long, and C. Ma, "Effect of subsequent curing on surface permeability and compressive strength of steam-cured concrete," *Construction and Building Materials*, vol. 188, pp. 424–432, 2018.

[9] G. Lin, Y. Liu, and Z. Xang, "Numerical modeling for predicting service life of reinforced concrete structures exposed to chloride environments," *Cement and Concrete Research*, vol. 32, no. 8, pp. 571–579, 2010.

[10] Q. Zhu, L. Jiang, and Y. Chen, "Effect of chloride salt type on chloride binding behavior of concrete," *Construction and Building Materials*, vol. 37, pp. 512–517, 2012.

[11] P. Brown and J. Bothe, "The system CaO-Al_2O_3-$CaCl_2$-H_2O at 23±2 °C and the mechanisms of chloride binding in concrete," *Cement and Concrete Research*, vol. 34, no. 9, pp. 1549–1553, 2009.

[12] B. M. Pérez, H. Zibara, R. D. Hooton, and M. D. A. Thomas, "A study of the effect of chloride binding on service life predictions," *Cement and Concrete Research*, vol. 30, no. 8, pp. 1215–1223, 2000.

[13] B. Reddy, G. K. Glass, and P. J. Lim, "On the corrosion risk presented by chloride bound in concrete," *Cement and Concrete Composites*, vol. 24, no. 1, pp. 1–5, 2002.

[14] M. A. Climent, G. de Vera, and J. F. López, "A test method for measuring chloride diffusion coefficients through non-saturated concrete: Part I. The instantaneous plane source diffusion case," *Cement and Concrete Research*, vol. 32, no. 7, pp. 1113–1123, 2002.

[15] Z. Jin, W. Sun, T. Zhao, and Q. Li, "Chloride binding in concrete exporse to corrosive solution," *Journal of the Chinese Ceramic Society*, vol. 37, no. 7, pp. 1068–1078, 2009, in Chinese.

[16] T. Cheewaket, C. Jaturapitakkul, and W. Chalee, "Long term performance of chloride binding capacity in fly ash concrete in a marine environment," *Construction and Building Materials*, vol. 24, no. 8, pp. 1352–1357, 2010.

[17] Z. Shi, M. R. Geiker, and K. D. Weerd, "Role of calcium on chloride binding in hydrated Portland cement-metakaolin-limestone blends," *Cement and Concrete Research*, vol. 95, pp. 205–216, 2017.

[18] C. Arya, N. R. Buenfeld, and J. B. Newman, "Factors influencing chloride-binding in concrete," *Cement and Concrete Research*, vol. 20, no. 2, pp. 291–300, 1990.

[19] H. Y. Moon, H. S. Kim, and D. S. Choi, "Relationship between average pore diameter and chloride diffusivity in various concretes," *Construction and Building Materials*, vol. 20, no. 9, pp. 725–732, 2006.

[20] Z. Yu, J. Ma, and G. Ye, "Effect of fly ash on the pore structure of cement paste under a curing period of 3 years," *Construction and Building Materials*, vol. 144, pp. 493–501, 2017.

[21] J. Zhang, J. Guo, and D. Li, "The influence of admixture on chloride time-varying diffusivity and microstructure of concrete by low-field NMR," *Ocean Engineering*, vol. 142, pp. 94–101, 2017.

[22] L. J. Malvar and L. R. Lenke, "Efficiency of fly ash in mitigating alkali-silica reaction based on chemical composition," *ACI Materials Journal*, vol. 103, no. 5, pp. 319–326, 2006.

[23] A. N. Givi, S. A. Rashid, F. N. A. Aziz, and M. A. M. Salleh, "Contribution of rice husk ash to the properties of mortar and concrete: A review," *Journal of American Science*, vol. 6, no. 3, pp. 157–165, 2010.

[24] C. S. Poon, S. C. Kou, and L. Lam, "Compressive strength, chloride diffusivity and pore structure of high performance metakaolin and silica fume concrete," *Construction and Building Materials*, vol. 20, no. 10, pp. 858–865, 2006.

[25] S. Caré, "Influence of aggregates on chloride diffusion coefficient into mortar," *Cement and Concrete Research*, vol. 33, no. 7, pp. 1021–1028, 2003.

[26] P. Sandberg, "Studies of chloride binding in concrete exposed in a marine environment," *Cement and Concrete Research*, vol. 29, no. 4, pp. 473–477, 1999.

[27] Y. Wang, Q. Li, and C. Lin, "Chloride diffusion analysis of concrete members considering depth-dependent diffusion coefficients and effect of reinforcement presence," *Journal of Materials in Civil Engineering*, vol. 28, no. 5, pp. 1–9, Article ID 04015183, 2016.

[28] M. D. A. Thomas and P. B. Bamforth, "Modelling chloride diffusion in concrete: Effect of fly ash and slag," *Cement and Concrete Research*, vol. 29, no. 4, pp. 487–495, 1999.

[29] B. H. Oh and S. Y. Jang, "Effects of material and environmental parameters on chloride penetration profiles in concrete structures," *Cement and Concrete Research*, vol. 37, no. 1, pp. 47–53, 2007.

[30] J. Liu, G. Ou, and Q. Qiu, "Chloride transport and microstructure of concrete with/without fly ash under atmospheric chloride condition," *Construction and Building Materials*, vol. 146, pp. 493–501, 2017.

[31] A. Petcherdchoo, "Time dependent models of apparent diffusion coefficient and surface chloride for chloride transport in fly ash concrete," *Construction and Building Materials*, vol. 38, pp. 497–507, 2013.

[32] A. K. Parande, B. R. Babu, and K. Pandi, "Environmental effects on concrete using Ordinary and Pozzolana Portland cement," *Construction and Building Materials*, vol. 25, no. 1, pp. 288–297, 2011.

[33] A. R. Boga and İ. B. Topcu, "Influence of fly ash on corrosion resistance and chloride ion permeability of concrete," *Construction and Building Materials*, vol. 31, pp. 258–264, 2012.

[34] T. Seo, M. Lee, C. Choi, and Y. Ohno, "Properties of drying shrinkage cracking of concrete containing fly ash as partial replacement of fine aggregate," *Magazine of Concrete Research*, vol. 62, no. 6, pp. 427–433, 2010.

[35] K. Isimaru, H. Mizuguchi, C. Hashimoto, and T. Ueda, "Properties of concrete using copper slag and second class fly ash as a part of fine aggregate," *Journal of the Society of Materials Science*, vol. 55, no. 8, pp. 828–833, 2005.

[36] China Academy of Building Research, *Standard for Test Method of Mechanical Properties on Ordinary concrete(GB/T 50081-2002)*, China Architecture and Building Press, Beijing, China, 2002.

[37] China Academy of Building Research, *Texting Code of Concrete for Port and Waterwog Engineering(JTG 270-98)*, China Architecture and Building Press, Beijing, China, 1999.

[38] T. U. Mohammed and H. Hamada, "Relationship between free chloride and total chloride contents in concrete," *Cement and Concrete Research*, vol. 33, no. 9, pp. 1487–1490, 2003.

[39] S. Muthulingam and B. N. Rao, "Chloride binding and time-dependent surface chloride content models for fly ash concrete," *Frontiers of Structural and Civil Engineering*, vol. 10, no. 1, pp. 112–120, 2016.

[40] T. Luping and L. O. Nilsson, "Chloride binding capacity and binding isotherms of OPC pastes and mortars[J]. Cement and concrete research," *Cement and Concrete Research*, vol. 23, no. 2, pp. 247–253, 1993.

[41] S. Sahu, S. Badger, and N. Thaulow, "Evidence of thaumasite formation in Southern California concrete," *Cement ang Concrete Composites*, vol. 24, no. 3, pp. 379–384, 2002.

[42] Y. Elakneswaran, T. Nawa, and K. Kurumisawa, "Electrokinetic potential of hydrated cement in relation to adsorption of chlorides," *Cement and Concrete Research*, vol. 39, no. 4, pp. 340–344, 2009.

[43] M. D. A. Thomsa and P. B. Bamforth, "Modelling chloride diffusion in concrete: Effect of fly ash and slag," *Cement and Concrete Research*, vol. 29, no. 9, pp. 487–495, 1999.

[44] M. V. A. Florea and H. J. H. Brouwers, "Chloride binding related to hydration products: Part I: Ordinary Portland Cement," *Cement and Concrete Research*, vol. 42, no. 2, pp. 282–290, 2012.

[45] H. Hirao, K. Yamada, and H. Takahashi, "Chloride binding of cement estimated by binding isotherms of hydrates," *Journal of Advanced concrete Technology*, vol. 3, no. 1, pp. 77–84, 2005.

[46] S. O. Ekolu, M. D. A. Thomas, and R. D. Hooton, "Pessimum effect of externally applied chlorides on expansion due to delayed ettringite formation: Proposed mechanism," *Cement and Concrete Research*, vol. 36, no. 4, pp. 688–696, 2006.